Journal of Food and Drug Analysis

Volume 26 | Issue 2 Article 35

Sialoglycoprotein isolated from eggs of Carassius auratus promotes fracture healing in osteoporotic mice

Available online at www.sciencedirect.com

ScienceDirect

journal homepage: www.jfda-online.com

Original Article

Sialoglycoprotein isolated from eggs of *Carassius auratus* promotes fracture healing in osteoporotic mice

Fei Wang, Lihua Han, Xiaohong Wang, Yuanyuan Li, Yujie Zhu, Jingfeng Wang, Changhu Xue*

College of Food Science and Engineering, Ocean University of China, Qingdao, Shandong Province, China

ARTICLE INFO

Article history:
Received 9 January 2017
Received in revised form
22 July 2017
Accepted 24 July 2017
Available online 22 September 2017

Keywords:
Carassius auratus eggs
Sialoglycoprotein
OVX
Fracture healing
Endochondral ossification

ABSTRACT

In this study, open tibial fracture surgery was performed on mice with ovariectomy induced osteoporosis to investigate the effect of a treatment with sialoglycoprotein isolated from *Carassius auratus* eggs (*Ca*-SGP) on fracture healing. Dynamic histological analysis showed that *Ca*-SGP promoted the generation of cartilage callus on day 5 post-surgery, then facilitated the transformation of the cartilage callus to bony callus on days 11 and 24 post-surgery, and enhanced the remodeling of bony callus on 35 day post-surgery. Moreover, *Ca*-SGP significantly decreased the secretion of TNF-α and IL-1β in serum on day 5 post-surgery, thus inhibiting the negative spread of the inflammatory reaction. On day 11 post-surgery, *Ca*-SGP clearly decreased the serum level and the mRNA expression of Aggrecan but also increased the secretion and the expression of VEGF and MMP13, thus promoting the degradation of the cartilage matrix and vascular invasion. On day 24 post-surgery, *Ca*-SGP remarkably increased the mRNA expression of osteogenesis markers Col1a and OCN, and increased callus BV/TV and Tb.N, this facilitating the formation of woven bone. On day 35 post-surgery, *Ca*-SGP enhanced the transformation of woven bone into lamellar bone and improved the callus biomechanical property. In conclusion, *Ca*-SGP promoted fracture healing in osteoporotic mice by accelerating endochondral ossification.

1. Introduction

Osteoporosis affects hundreds of millions of people worldwide, and is characterized by low bone density and strength, high bone fragility with consequent susceptibility to fracture [1,2]. Osteoporosis and osteoporosis-related fractures are currently the major causes of morbidity and mortality among the elderly [3]. Numerous studies have reported that

Abbreviations: Ca-SGP, sialoglycoprotein isolated from eggs of *Carassius auratus*; ALN, alendronate sodium; IL-1β, interleukin 1β; VEGF, vascular endothelial growth factor; MMP13, matrix metallopeptidase 13; Col10a, collagen type X; Col1a, collagen type I; OCN, osteocalcin.

* *Corresponding author*. Fax: +86 0532 82032468.
E-mail address: jfwang@ouc.edu.cn (J. Wang).

https://doi.org/10.1016/j.jfda.2017.07.017

osteoporosis could result in not only delayed fracture healing but also in disturbed callus formation with decreased bone mineral density, and volume, and altered biomechanical properties [4–6]. Ovarian hormone deficiency is a key risk factor for postmenopausal osteoporosis. Estrogen has been reported to enhance fracture healing in mice thanks to its effect on the regulation of skeletal growth, development and maintenance, as well as on the cartilage homeostasis, growth, and maturation [7,8].

Currently, some anti-resorptive drugs such as bisphosphonates, estrogen, selective estrogen receptor modulators and calcitonin, have been used to promote callus formation during fracture healing [9,10]. However, these existing therapeutic options are limited not only due to their inherent adverse effects, but also because of the delay that they imply in bone remodeling at the late healing stage. Thus, the identification of novel alternatives for the treatment of osteoporotic fracture is urgently needed. Sialoglycoproteins (SGPs) belong to the family of highly acidic glycoproteins and can be found in the eggs of many vertebrates [11]. Fish eggs are one of the major byproducts of the fish-processing industry and can be easily retrieved. In our previous work, sialoglycoprotein was successfully isolated from the eggs of *Carassius auratus* (*Ca*-SGP), and its anti-osteoporotic effect was demonstrated using ovariectomized (OVX) rats and the senescence-accelerated mouse strain P6 *in vivo* [12–14].

Fracture healing involves a well-characterized cascade of events including three major phases: the reactive phase, the reparative phase, and the remodeling phase. Endochondral ossification is identified as an indispensable process for reparative phase in fracture healing [15,16]. It begins with mesenchymal stem cell condensation, followed by chondrocyte proliferation, differentiation, maturation, and apoptosis, as well as vasculature invasion of the fracture site. In this study, in order to explore the value of *Ca*-SGP use on bone metabolism, open tibial fracture surgery was performed on mice with OVX-induced osteoporosis to investigate the effect of a *Ca*-SGP treatment on fracture healing.

2. Materials and methods

2.1. Materials and reagents

Fresh female *C. auratus* were purchased at a seafood market in Qingdao, China. The ovaries were quickly taken out under an ice bath. After removing the egg envelope, the fish eggs were extracted and stored at −80 °C until use.

Moloney murine leukemia virus reverse transcriptase (M-MLV), dNTPs, random primer, and PageRuler prestained protein ladder were procured from TaKaRa Bio Inc. (Otsu, Shiga, Japan). FastStart Universal SYBR Green Master (Rox) was purchased from Roche (Roche Applied Science, Mannheim, Germany). The primers of genes including Aggrecan, collagen type X(Col10a), vascular endothelial growth factor (VEGF), matrix metallopeptidase 13 (MMP13), collagen type I(Col1a) and osteocalcin (OCN) were synthesized by Sangon Biotech Co. Ltd. (Shanghai, China).

2.2. Preparation of Ca-SGP

Ca-SGP was prepared as previously reported [14]. Its purity was 94.76%, and its molecular weight 195.35 kDa. *Ca*-SGP contained 62.81% hexose, 14.33% protein, and 19.72% N-acetylneuraminic acid. Monosaccharide composition analysis showed the presence of mannose, glucosamine, galactosamine, and galactose with a molar ratio of 1:2.98:2.65:5.09.

2.3. Animals and experimental design

This study was approved by the Ethics Committee of Experimental Animal Care at the Ocean University of China (certificate no. SYXK20120014). Nine-week-old female C57BL/6J mice (20 ± 2.0 g) were purchased from the Vital River Laboratory Animal Center (Beijing, China; license ID SCXK2012-0001). The animals were housed four per cage at 23 ± 1 °C with a 12 h light/12 h dark cycle and they were given food and water ad libitum. After 7 days of acclimatization, the animals were sham-operated (control, n = 54) or subjected to bilateral ovariectomy (n = 150) and then left untreated for 10 weeks to allow bone loss. The femurs of six mice were collected in each group to demonstrate the successful establishment of the osteoporotic model using histological analysis. Then the OVX animals were randomly allocated to one of the three following groups (n = 48 per group): a model group (treated with physiological saline), an OVX + ALN group (treated with alendronate sodium as a positive control; 1 mg/kg body weight) and an OVX + *Ca*-SGP group (treated with *Ca*-SGP; 500 mg/kg body weight). The control group was also treated with physiological saline. In each group, animals were given intragastric administration of either physiological saline or their respective drugs (1 mL/100 g body weight) once a day. After 7 days of treatment, all the animals were subjected to an open fracture operation according to the method described in Ref. [17], with slight modifications. Briefly, a transverse osteotomy was made at the proximal third of the right tibia diaphysis under general anesthesia and sterile conditions. Then, the patella was laterally deflected and a hole was drilled through the intercondylar eminence of the tibia. Subsequently, the fracture site was connected by a 0.45-mm Kirschner wire inserted through the hole across the fracture ends. The locations of the fracture and the inserted Kirschner wire were monitored by a HY-450DR X-ray system (KangDa, Shanghai, China) after operation. Drug administration was continued after fracture surgery.

Serum was dynamically collected on days 3, 5 and 11 post-surgery for the determination of biochemical indicators (n = 8 per group). Tibiae callus (n = 6 per group) collected days 5, 11, 24 and 35 post-surgery were used for histological analysis. Similarly, six tibial calluses per group were collected for a micro-CT analysis on day 24 post-surgery, for a biomechanical property testing on day 35 post-surgery, and for the measurement of mRNA expression on days 11 and 24 post-surgery.

2.4. Determination of serum biochemical indicators

The biochemical indicators including TNF-α, interleukin 1β (IL-1β), VEGF, Aggrecan and MMP13 in serum were measured using commercial ELISA kits (R&D Systems, Minneapolis, MN, USA).

2.5. Histological analysis and bone biomechanical testing

The distal femur or the tibial callus was fixed in 10% neutral formaldehyde for 24 h and then decalcified in 10% EDTA for 3 weeks. The decalcified tissues were then embedded in paraffin after dehydration with ascending grades of ethanol. The embedded samples were serially sectioned (thickness = 4 μm) and stained with hematoxylin and eosin (H&E). Tibial callus stiffness was measured using YLS-16A bone strength tester (Yiyan, China).

2.6. Micro-CT analysis

After removal of soft tissues and the intramedullary pin, the collected tibiae were scanned by a micro-CT system (μCT80 scanner, Scanco Medical AG, Bassersdorf, Switzerland) at a voltage of 70 kV with a current of 114 μA. The scan range covered a distance between 3 mm proximal and 3 mm distal to the fracture line with a resolution of 10 μm, this allowing to calculate morphometric parameters including the bone volume ratio (BV/TV), the trabecular number (Tb.N) and the trabecular separation (Tb.Sp). The transverse section of the callus obtained from 2D CT images was analyzed using ImageJ software.

2.7. Real-time PCR

The mRNA expression of genes was measured by real-time PCR. The RNA extraction and amplification were performed according to the method previously described in Ref. [18], with slight modifications. Briefly, the callus tissue was grounded into powder with liquid nitrogen, then total RNA was extracted using TRIzol reagent, and 1 μg of RNA was reverse transcribed to cDNA by M-MLV reverse transcriptase. Twenty-five microliters of reaction system was applied for real-time PCR and consisted of 5 μL of template, 12.5 μL of FastStart Universal SYBR Green Master, 0.75 μL each of forward and reverse primers and 6 μL of sterile Milli-Q water. The thermal process consisted of an initial denaturation at 95 °C for 10 min followed by 45 cycles of denaturation at 95 °C for 15 s, annealing at 60 °C for 30 s, and extension at 72 °C for 30 s.

2.8. Statistical analysis

Data were submitted to a one-way analysis of variance (ANOVA) with SPSS statistical program, and significant differences among treatments were compared by the least significance difference (LSD) method multiple-range test. The results are presented as means with their standard deviation. In statistical analysis, values of $P < 0.05$ were considered as significant.

3. Results

3.1. Establishment of the osteoporotic fracture model

Ten weeks after OVX, H&E stain was applied to the paraffin sections of the distal femur to examine the changes in cancellous bone and bone marrow stroma. Fig. 1A shows that compared with the sham control group, OVX induced a reduction of bone trabecula under the growth plate and an increase of adipocytes in the marrow cavity, suggesting that the osteoporosis phenotype was observed in the model group. In addition, the location of the fracture and the inserted Kirschner wire observed by X-ray are shown in Fig. 1B.

3.2. The dynamic change of serum biochemical indicators

Fracture healing is accompanied by a cascade of events that begins with an inflammatory reaction. Fig. 2A shows that on day 3 post-surgery, the contents of TNF-α and IL-1β in serum were indistinguishable among the different groups. On day 5 post-surgery, the inflammatory reaction continued to increase in the model group, while the *Ca*-SGP treatment inhibited the further spread of the inflammation, as evidenced by the significantly reduced TNF-α and IL-1β levels in the OVX + *Ca*-SGP group. Fig. 2B shows that on day 11 post-surgery, the content of Aggrecan in the model group was obviously higher than that in the control group, while, in contrast, VEGF and MMP13 levels were lower. Compared with the model group, the *Ca*-SGP treatment remarkably decreased the secretion of Aggrecan and increased the level of MMP13 and VEGF, indicating that *Ca*-SGP promoted the degradation of the cartilage matrix and the invasion of blood vessel.

3.3. Ca-SGP promoted the generation of a cartilage callus

On day 5 post-surgery, a cartilage callus was observed around the fracture site in the control group. Moreover, the morphology of many chondrocytes was hypertrophic. Nevertheless, there was still a large amount of fibrous callus and hematoncus in the OVX model group, indicating that osteoporosis induced a delay for the mesenchymal stem cells to differentiate into chondrocytes. Interestingly, compared with the model group, the treatment with *Ca*-SGP promoted the generation of a cartilage callus, in spite of the fact that chondrocytes were immature and non-hypertrophic (Fig. 3).

3.4. Ca-SGP facilitated the transformation of cartilage callus into bony callus

H&E stain in Fig. 4A shows that on day 11 post-surgery, a large proportion of cartilage callus had been replaced by new bone tissue around the fracture site. However, in the model group, the callus was still at the peak of chondrocytes proliferation and hypertrophic differentiation. The *Ca*-SGP treatment accelerated the mineralization and the degradation of cartilage matrix and the invasion of vascular. The H&E stain shown in Fig. 4B indicates that on day 24 post-surgery, the formed woven bone in the control group was compact and inerratic, whereas there were few new bone tissue generated in the model group. Fortunately, the treatment with *Ca*-SGP facilitated the unceasing formation of woven bone around the fracture site. The micro-CT quantification analysis of bony

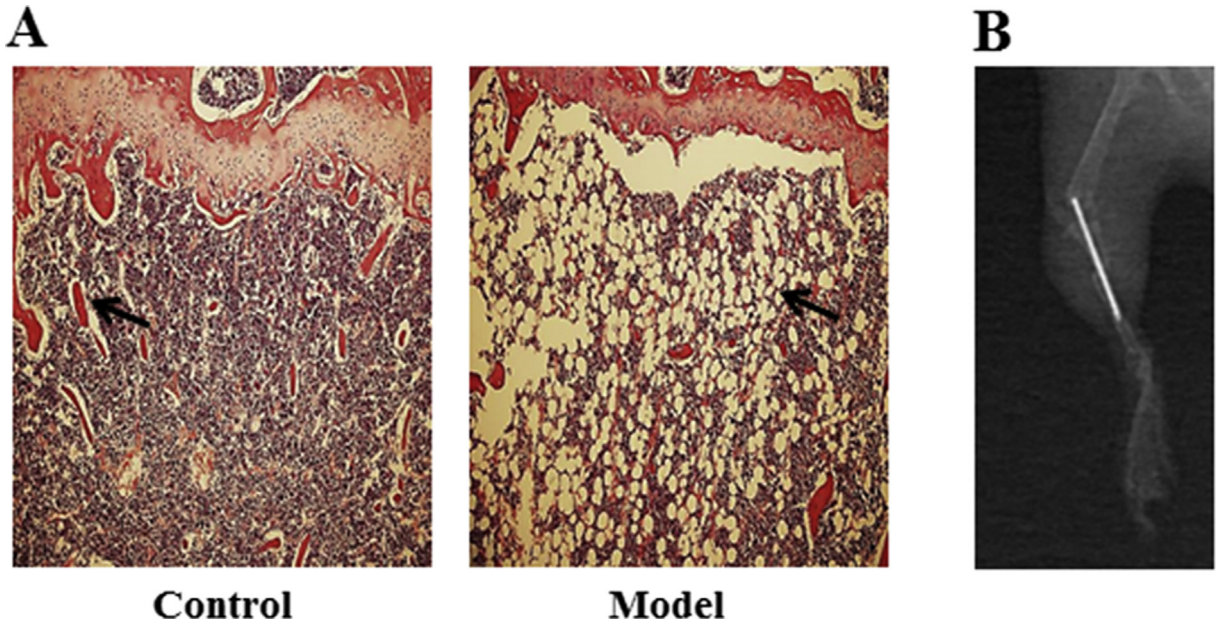

Fig. 1 – Establishment of the osteoporotic fracture model. A: H&E staining of the distal femur 10 weeks after OVX (n = 6). Distal femurs were fixed in 10% neutral formaldehyde for 24 h and then decalcified in 10% EDTA for 3 weeks. The decalcified tissues were embedded in paraffin after dehydration with ascending grades of ethanol. Then, the embedded samples were serially sectioned (thickness = 4 μm) and stained with hematoxylin and eosin (H&E). Finally, the tissue slices were observed and photographed using BH-2 microscope equipped with matching camera software (10 × magnification). B: X-ray testing of the right tibiae after fracture surgery. After fracture surgery, the locations of the fracture and the inserted Kirschner wire were immediately monitored by a HY-450DR X-ray system.

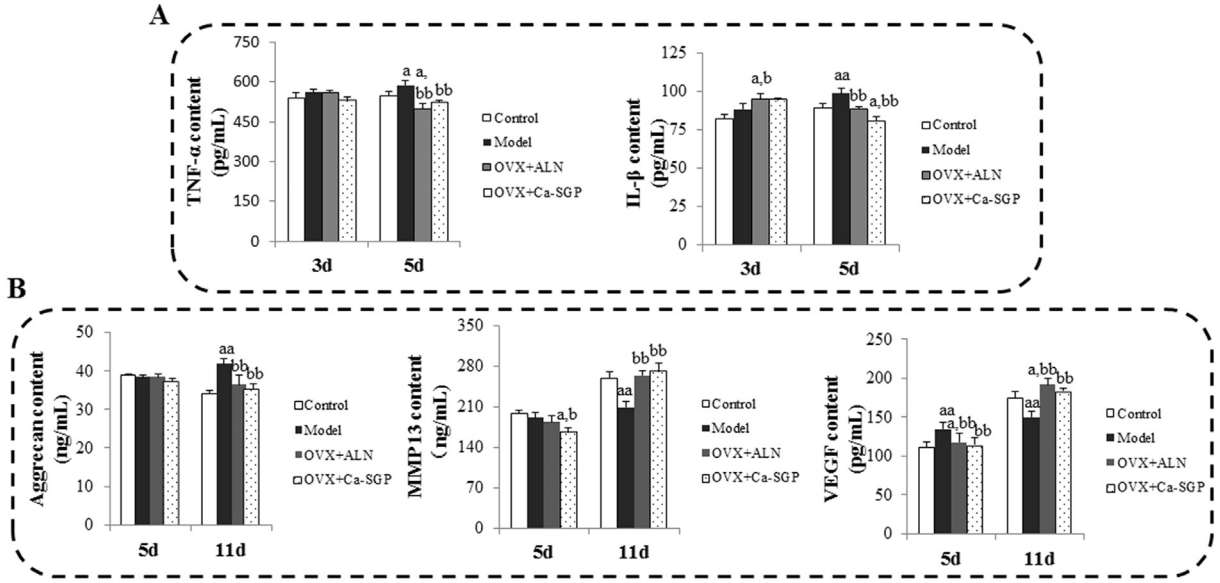

Fig. 2 – Effects of *Ca*-SGP on serum biochemical indicators. A: TNF-α and IL-1β contents on days 3 and 5 post-surgery. B: Aggrecan, VEGF, MMP13 contents on days 5 and 11 post-surgery. The biochemical indicators in serum were measured using commercial ELISA kits. Data are presented as mean ± SD (n = 8 per group). Multiple comparisons were done using one way ANOVA analysis. [a] P < 0.05, [aa] P < 0.01 versus control group; [b] P < 0.05, [bb] P < 0.01 versus model group.

callus on day 24 post-surgery further demonstrated that compared with the model group, *Ca*-SGP significantly increased BV/TV and Tb.N, and decreased the callus size and Tb.Sp, this promoting mineralization of the callus (Fig. 5).

3.5. *Ca-SGP enhanced the remodeling of the bony callus*

Following the transformation of cartilage callus into new bone tissue around the fracture site, the callus entered a stage of

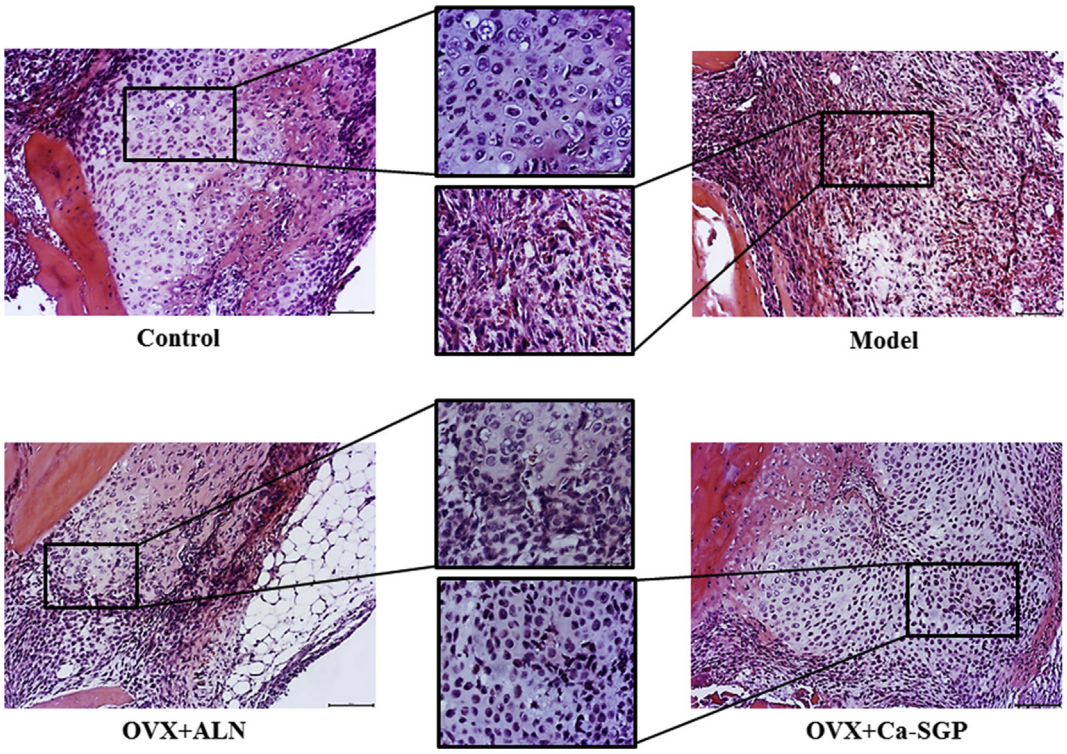

Fig. 3 – H&E staining of the callus on day 5 post-surgery. The calluses were fixed in 10% neutral formaldehyde for 24 h and then decalcified in 10% EDTA for 3 weeks. The decalcified tissues were embedded in paraffin after dehydration with ascending grades of ethanol. Then, the embedded samples were serially sectioned (thickness = 4 μm) and stained with H&E. Finally, the tissue slices were observed and photographed using BH-2 microscope equipped with matching camera software (n = 6, 10 × and 20 × magnification).

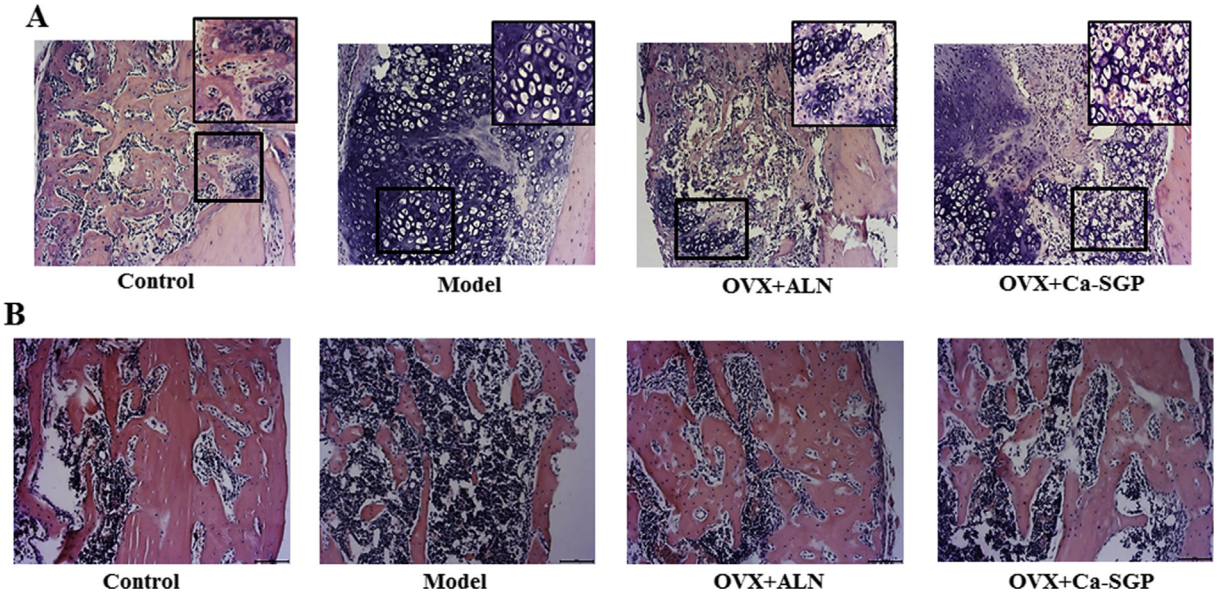

Fig. 4 – H&E staining of the callus on days 11 and 24 post-surgery. A: H&E staining of the callus on day 11 post-surgery (n = 6, 10 × and 20 × magnification). B: H&E staining of the callus on day 24 post-surgery (n = 6, 10 × magnification). The calluses were fixed in 10% neutral formaldehyde for 24 h and then decalcified in 10% EDTA for 3 weeks. The decalcified tissues were embedded in paraffin after dehydration with ascending grades of ethanol. Then, the embedded samples were serially sectioned (thickness = 4 μm) and stained with H&E. Finally, the tissue slices were observed and photographed using BH-2 microscope equipped with matching camera software.

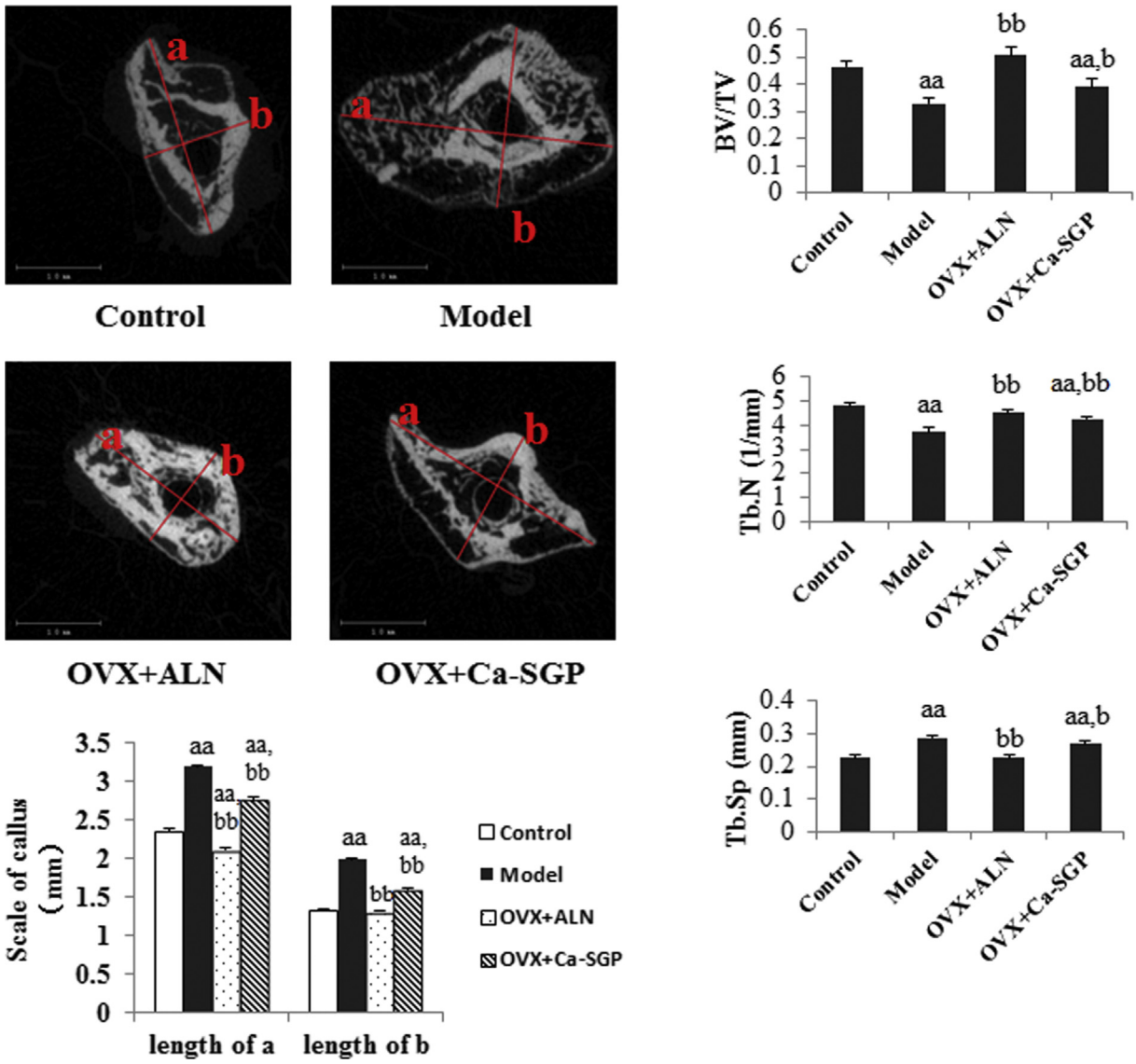

Fig. 5 – Micro-CT testing of the callus on day 24 post-surgery. After removal of soft tissues and the intramedullary pin, the collected tibiae were scanned by a micro-CT system at a voltage of 70 kV with a current of 114 μA. The scan range covered a distance between 3 mm proximal and 3 mm distal to the fracture line with a resolution of 10 μm and followed for the calculation of the following morphometric parameters: BV/TV, Tb.N and Tb.Sp. The transverse section of the callus obtained from 2D CT images was analyzed using ImageJ software. Data are presented as mean ± SD (n = 6 per group). Multiple comparisons were done using one way ANOVA analysis. ^{aa} $P < 0.01$ versus control group; ^{b} $P < 0.05$, ^{bb} $P < 0.01$ versus model group.

continuous bone remodeling to restore its original shape and function. On day 35 post-surgery, the callus was still made of woven bone in the model group, while lamellar bone was observed in the OVX + *Ca*-SGP group, suggesting that the treatment with *Ca*-SGP enhanced the bone remodeling capability around the fracture site (Fig. 6A). Moreover, the three-point bending test demonstrated that the *Ca*-SGP treatment significantly improved the callus stiffness by 48.35% compared with the model group (Fig. 6B).

3.6. Ca-SGP regulated the expression of key genes in endochondral ossification

Endochondral ossification requires the hypertrophic differentiation of chondrocytes and the conversion of cartilage tissue into bone tissue through the degradation of the cartilage matrix and vascular invasion [19]. The mRNA expression of chondrocyte proliferation marker Aggrecan, chondrocyte hypertrophic marker Col10a, cartilage matrix degradation

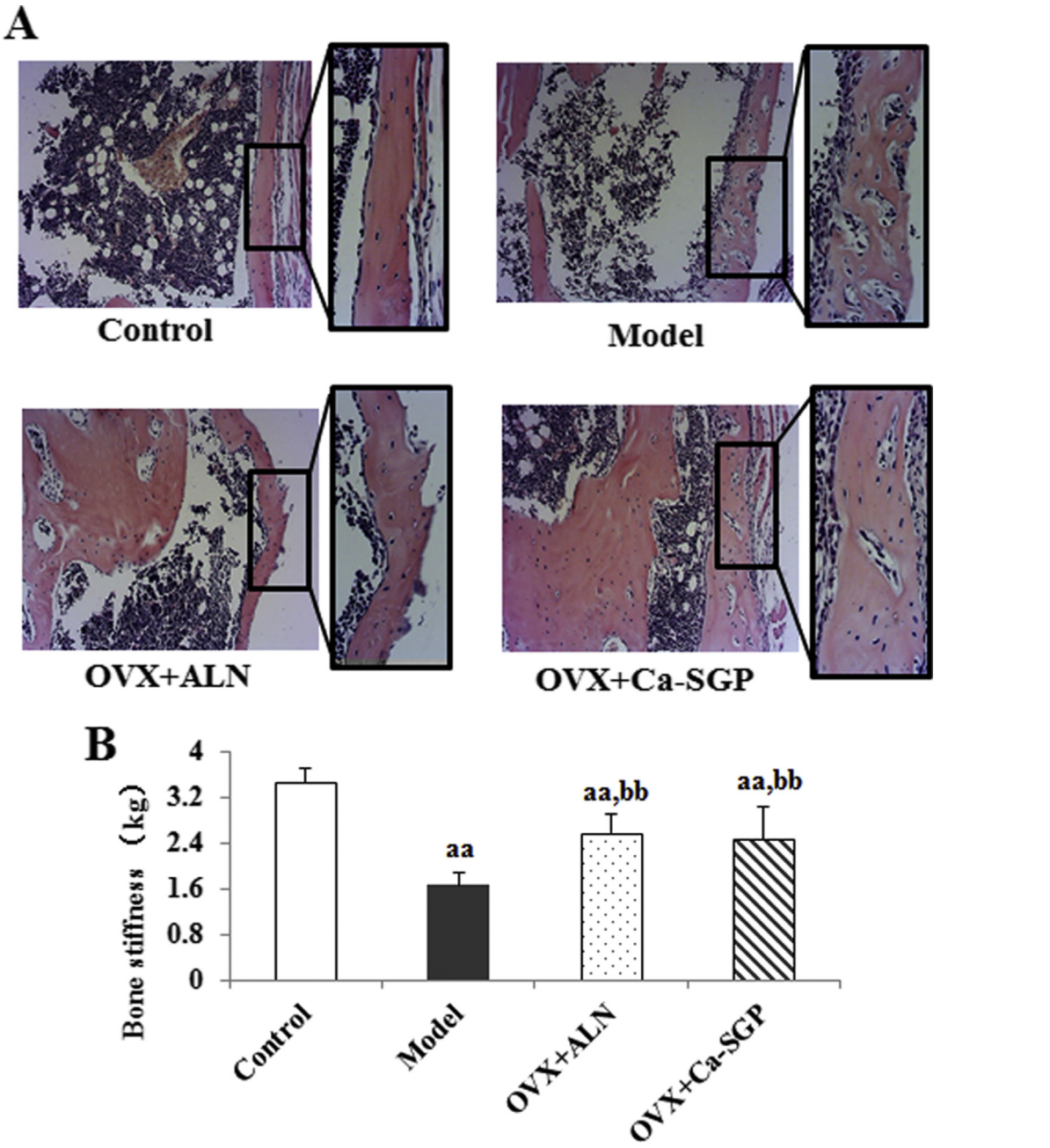

Fig. 6 – Callus H&E staining and stiffness testing on day 35 post-surgery. A: H&E staining of the callus (n = 6, 10 × and 20 × magnification). B: Callus stiffness. The tibial calluses were fixed in 10% neutral formaldehyde for 24 h and then decalcified in 10% EDTA for 3 weeks. The decalcified tissues were embedded in paraffin after dehydration with ascending grades of ethanol. Then, the embedded samples were serially sectioned (thickness = 4 μm) and stained with H&E. Finally, the tissue slices were observed and photographed using BH-2 microscope equipped with matching camera software. The tibial callus stiffness was measured using a YLS-16A bone strength tester. Data are presented as mean ± SD (n = 6 per group). Multiple comparisons were done using one way ANOVA analysis. ^{aa} P < 0.01 versus control group; ^{bb} P < 0.01 versus model group.

marker MMP13, vascularization marker VEGF and osteogenesis marker Col1a and OCN on days 11 and 24 post-surgery were determined. As shown in Fig. 7, overall, the mRNA expression levels of Aggrecan, Col10a, MMP13 and VEGF were decreased on day 24 post-surgery compared with day 11 post-surgery. In contrast, Col1a and OCN were increased, indicating the transformation of cartilage callus into bony callus with time. Specifically, the mRNA expression levels of Aggrecan and Col10a were clearly higher in the model group than in the control group, while the expression levels of MMP13, VEGF, Col1a and OCN were remarkably lower, in spite of the unapparent change in MMP13 on day 11 post-surgery. This suggests that our osteoporosis model retarded the conversion of hypertrophic cartilage tissue into new bone tissue. In contrast, *Ca*-SGP promoted the entochondrostosis process, as evidenced by the significantly decreased expression of Aggrecan

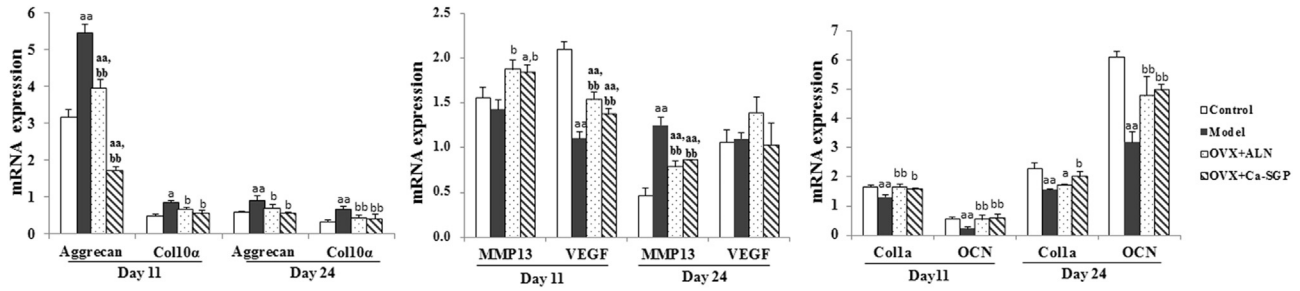

Fig. 7 – The mRNA expression of key genes on days 11 and 24 post-surgery. The callus tissue was grounded into powder with liquid nitrogen, then total RNA was extracted using TRIzol reagent, and reverse transcribed to cDNA by M-MLV reverse transcriptase. The mRNA expression of Aggrecan, Col10a, VEGF, MMP13, Col1a and OCN were examined using real-time PCR. Data are presented as mean ± SD (n = 6 per group). Multiple comparisons were done using one way ANOVA analysis. [a] $P < 0.05$, [aa] $P < 0.01$ versus control group; [b] $P < 0.05$, [bb] $P < 0.01$ versus model group.

and Col10a, and the increased expression of MMP13, VEGF, Col1a and OCN.

4. Discussion

In this study, we showed that *Ca*-SGP can promote tibia fracture healing in mice with OVX-induced osteoporosis by facilitating a generation of cartilage callus at the early stage of healing, improving the conversion of this cartilage callus into a bony callus at the middle stage, as well as improving the remodeling of bony callus at the later stage of healing.

Fracture healing is a complex regenerative process initiated in response to injury, which, in the best case, results in the restoration of the skeletal shape and function. In the initial phase of fracture repair, the undifferentiated mesenchymal cells and fibroblasts are aggregated at the injury site, then proliferate and differentiate, in response to inflammatory factors and other cytokines [20,21]. Along with the differentiation of the mesenchymal cells into chondrocytes, the secretion of inflammation factors are progressively suppressed [22]. On day 5 post-surgery, the serum contents of TNF-α and IL-1β in the model group were clearly higher than in the control group. Also, histological staining showed that there were still numerous hematoncus and fibrous tissue at the injury site in the model group instead of cartilage tissue in the control group, indicating that the continued spread of inflammatory reaction in the model group inhibited the generation of cartilage callus around the fracture site. In addition, the higher serum level of VEGF in the model group also reflects that the hypoxia status induced by the injury was not timely alleviated [23]. The treatment with *Ca*-SGP significantly decreased the secretion of TNF-α, IL-1β and VEGF, and promoted the formation of a cartilage callus.

Once cartilage matrix is produced, the steps of chondrocyte hypertrophy, cartilage degradation and vascular invasion are well coordinated to further transform this cartilage into bone tissue. Aggrecan is a cartilage matrix protein, whereas Col10a is a chondrocyte hypertrophy marker, the degradation of cartilage matrix requires MMP13, while the vascular invasion depends on VEGF [19,24–26]. On day 11 post-surgery, H&E staining revealed that a large proportion of the cartilage tissue was replaced by new bone tissue in the control group but not in the model group, while *Ca*-SGP enhanced the matrix mineralization and vascular invasion. In the same time, *Ca*-SGP significantly decreased the serum content and the mRNA expression of Aggrecan, increased the secretion and expression levels of MMP13 and VEGF, as well as the mRNA expression of the osteogenesis marker Col1a and OCN. This further confirmed the beneficial effect of *Ca*-SGP on the osteoporosis-induced delay in endochondral ossification.

On day 24 post-surgery, the process of endochondral ossification was completed, and the callus entered a continuous remodeling period as shown in the histological staining of the callus (see Fig. 4B). The increased number of woven bone on day 24 post-surgery, the enhanced formation of lamellar bone as well as the improved callus stiffness on day 35 post-surgery in the OVX + *Ca*-SGP group demonstrated that *Ca*-SGP promoted the restoration of skeletal shape and function. In addition, compared with the model group, the *Ca*-SGP treatment significantly increased the mRNA expression of osteogenesis-associated genes including Col1a and OCN, thus confirming that *Ca*-SGP enhanced the later bone remodeling. In conclusion, *Ca*-SGP promoted fracture healing in osteoporotic mice by accelerating endochondral ossification.

As a novel bioactive compound, *Ca*-SGP has been demonstrated to inhibit osteoclasts activity, promote differentiation and mineralization of osteoblasts *in vitro*, and ameliorate osteoporosis *in vivo* [12–14,27]. This study further showed that *Ca*-SGP exhibits fracture healing improving effect in osteoporotic mice. These studies may provide some theoretical basis for the exploitation of functional foods or drugs to preserve bone metabolism, and achieve the high-value application of fish eggs in future.

Funding

This study is financially supported by National Natural Science Foundation of China (No. 31371876 and No. 31571771).

Conflicts of interest statement

The authors declare no competing financial interest.

Appendix A. Supplementary data

Supplementary data related to this article can be found at https://doi.org/10.1016/j.jfda.2017.07.017.

REFERENCES

[1] Kanis JA, McCloskey EV, Johansson H, Cooper C, Rizzoli R, Reginster JY. European guidance for the diagnosis and management of osteoporosis in postmenopausal women. Osteoporos Int 2013;24:23–57.

[2] Baron R, Kneissel M. WNT signaling in bone homeostasis and disease: from human mutations to treatments. Nat Med 2013;19:179–92.

[3] Li W, Wang K, Liu Z, Ding W. HIF-1alpha change in serum and callus during fracture healing in ovariectomized mice. Int J Clin Exp Pathol 2015;8:117–26.

[4] Namkung-Matthai H, Appleyard R, Jansen J, Hao Lin J, Maastricht S, Swain M, et al. Osteoporosis influences the early period of fracture healing in a rat osteoporotic model. Bone 2001;28:80–6.

[5] McCann RM, Colleary G, Geddis C, Clarke SA, Jordan GR, Dickson GR, et al. Effect of osteoporosis on bone mineral density and fracture repair in a rat femoral fracture model. J Orthop Res 2008;26:384–93.

[6] Hao YJ, Zhang G, Wang YS, Qin L, Hung WY, Leung K, et al. Changes of microstructure and mineralized tissue in the middle and late phase of osteoporotic fracture healing in rats. Bone 2007;41:631–8.

[7] He YX, Liu Z, Pan XH, Tang T, Guo BS, Zheng LZ, et al. Deletion of estrogen receptor beta accelerates early stage of bone healing in a mouse osteotomy model. Osteoporos Int 2012;23:377–89.

[8] Beil FT, Barvencik F, Gebauer M, Seitz S, Rueger JM, Ignatius A, et al. Effects of estrogen on fracture healing in mice. J Trauma 2010;69:1259–65.

[9] Cao Y, Mori S, Mashiba T, Westmore MS, Ma L, Sato M, et al. Raloxifene, estrogen, and alendronate affect the processes of fracture repair differently in ovariectomized rats. J Bone Miner Res 2002;17:2237–46.

[10] Li X, Luo X, Yu N, Zeng B. Effects of salmon calcitonin on fracture healing in ovariectomized rats. Saudi Med J 2007;28:60–4.

[11] Inoue S, Inoue Y. Chapter 7-Fish glycoproteins. In: Montreuil JFGVJ, Schachter H, editors. New comprehensive biochemistry. Elsevier; 1997. p. 143–61.

[12] Wang F, Wang Y, Zhao Y, Zhan Q, Yu P, Wang J, et al. Sialoglycoprotein isolated from eggs of *Carassius auratus* ameliorates osteoporosis: an effect associated with regulation of the Wnt/beta-Catenin pathway in rodents. J Agric Food Chem 2016;64:2875–82.

[13] Xia G, Wang J, Sun S, Zhao Y, Wang Y, Yu Z, et al. Sialoglycoproteins prepared from the eggs of *Carassius auratus* prevent bone loss by inhibiting the NF-kappaB pathway in ovariectomized rats. Food Funct 2016;7:704–12.

[14] Xia G, Wang S, He M, Zhou X, Zhao Y, Wang J, et al. Anti-osteoporotic activity of sialoglycoproteins isolated from the eggs of *Carassius auratus* by promoting osteogenesis and increasing OPG/RANKL ratio. J Func Foods 2015;15:137–50.

[15] Bahney CS, Hu DP, Miclau T, Marcucio RS. The multifaceted role of the vasculature in endochondral fracture repair. Front Endocrinol 2015;6:4.

[16] Kozhemyakina E, Lassar AB, Zelzer E. A pathway to bone: signaling molecules and transcription factors involved in chondrocyte development and maturation. Development 2015;142:817–31.

[17] Li YF, Zhou CC, Li JH, Luo E, Zhu SS, Feng G, et al. The effects of combined human parathyroid hormone (1-34) and zoledronic acid treatment on fracture healing in osteoporotic rats. Osteoporos Int 2012;23:1463–74.

[18] Hu S, Xia G, Wang J, Wang Y, Li Z, Xue C. Fucoidan from sea cucumber protects against high-fat high-sucrose diet-induced hyperglycaemia and insulin resistance in mice. J Func Foods 2014;10:128–38.

[19] Saito T, Fukai A, Mabuchi A, Ikeda T, Yano F, Ohba S, et al. Transcriptional regulation of endochondral ossification by HIF-2alpha during skeletal growth and osteoarthritis development. Nat Med 2010;16:678–86.

[20] Hankenson KD, Gagne K, Shaughnessy M. Extracellular signaling molecules to promote fracture healing and bone regeneration. Adv Drug Deliv Rev 2015;94:3–12.

[21] Chen Y, Whetstone HC, Lin AC, Nadesan P, Wei Q, Poon R, et al. Beta-catenin signaling plays a disparate role in different phases of fracture repair: implications for therapy to improve bone healing. PLoS Med 2007;4:e249.

[22] Kon T, Cho TJ, Aizawa T, Yamazaki M, Nooh N, Graves D, et al. Expression of osteoprotegerin, receptor activator of NF-kappaB ligand (osteoprotegerin ligand) and related proinflammatory cytokines during fracture healing. J Bone Miner Res 2001;16:1004–14.

[23] Lienau J, Schmidt-Bleek K, Peters A, Haschke F, Duda GN, Perka C, et al. Differential regulation of blood vessel formation between standard and delayed bone healing. J Orthop Res 2009;27:1133–40.

[24] Ortega N, Behonick DJ, Werb Z. Matrix remodeling during endochondral ossification. Trends Cell Biol 2004;14:86–93.

[25] Stickens D, Behonick DJ, Ortega N, Heyer B, Hartenstein B, Yu Y, et al. Altered endochondral bone development in matrix metalloproteinase 13-deficient mice. Development 2004;131:5883–95.

[26] Zelzer E, Mamluk R, Ferrara N, Johnson RS, Schipani E, Olsen BR. VEGFA is necessary for chondrocyte survival during bone development. Development 2004;131:2161–71.

[27] Xia G, Yu Z, Zhao Y, Wang Y, Wang S, He M, et al. Sialoglycoproteins isolated from the eggs of *Carassius auratus* prevents osteoporosis by suppressing the activation of osteoclastogenesis related NF-κB and MAPK pathways. J Func Foods 2015;17:491–503.